AN INVESTIGATION OF THE EFFECT OF TWIST ON THE COUPLED BENDING-TORSION VIBRATIONS OF A CANTILEVER BEAM

GEORGE J. KLETT,
MICHAEL S. SHUTTY

1959

AN INVESTIGATION OF THE EFFECT OF TWIST ON THE COUPLED BENDING-TORSION VIBRATIONS OF A CANTILEVER BEAM

by

Lt. George J. Klett USN
//

and

Lt. Michael S. Shutty USN

AN INVESTIGATION OF THE EFFECT OF TWIST ON THE COUPLED BENDING-TORSION VIBRATIONS OF A CANTILEVER BEAM

SUMMARY

An experimental study was made of the effect of twist on the natural frequencies, coupled in bending and torsion, of a cantilever beam. The shape of the beam was selected to provide a high degree of coupling. An analytic procedure for determining these frequencies was also developed and is included in this report.

It was determined that coupling without twist reduced all frequencies from their uncoupled values. The fundamental frequency was found to remain relatively constant as the beam was twisted. All natural frequencies higher than the fundamental were lowered as the total twist was increased to 15 degrees, but remained relatively constant with further twist.

INTRODUCTION

With the advance of helicopters and turbo-machinery, the problem of twist and its effect upon the natural vibrations of a beam becomes of more and more interest. Much work has been done to determine the effect of twist on beams having no coupling between torsion and bending, and the effect of a high degree of bending-torsion coupling on untwisted beams. This report shows primarily the effect of twist on the natural frequencies of a particular beam highly coupled in bending and torsion. It also shows the node lines for all the natural frequencies, and indicates the effect of bending-torsion coupling on the natural frequencies in the untwisted beam.

A beam with dimensions as shown in Fig. 1 is considered. This particular shape was chosen to give a maximum amount of bending-torsion coupling, relatively easy tooling problems, and readily obtainable sectional and elastic properties. In this report, the term coupling refers to the interaction of the torsional, flapwise bending, and chordwise bending types of vibrations. It was planned to use both experimental tests and analytic means to determine the natural frequencies resulting from the combination of twist and coupling. Only experimental results however, are contained in this report. Difficulties encountered in preparing the digital computer program prevented the inclusion of analytic results. The mathematical method used is outlined in the Appendix.

This method is based on one being used in a report of Isakson and Eisley currently being prepared for the University of Michigan Research Institute. It involves the introduction of coupling terms from the equations of motion developed

by Houbolt and Brooks, Ref. 1, into the matrix method of solution of Targoff, Ref. 2 &3. The Targoff method was described and used in a report of Isakson and Eisley, Ref. 4.

The coordinate system used is shown in Fig. 2. The flexural center of the cross section was located according to a formula from Roark. Ref. 5, which formula was developed from Ref. 7. The elastic axis of the beam was maintained as a straight line by mechanically twisting the beam about this axis. The nomenclature and sign convention for the displacements, shears and bending moments used in the analysis are shown in Fig. 2. All parameters used or needed are listed in the table of symbols. The non-dimensional forms of these parameters used in the analysis are also listed in the table of symbols. The mass and stiffness distributions are uniform for the length of the beam.

In gathering the experimental data, tests were made at total angles of twist of 0^{o}, 5.5^{o}, 7.90, 12.9^{o}, 20.7^{o}, 26.7^{o}, 30.4^{o}, and 40.8^{o}.

In conducting this investigation, the assistance and guidance of Professors Eisley and Isakson, of the Department of Aeronautical Engineering of the University of Michigan, were of great value.

SYMBOLS

A	$GJ + EB_1 \times (\beta')^2$
$\bar{A}$	$\frac{A}{EI_1}$
B_1	cross section constant $\int_{\eta_{te}}^{\eta_{le}} t\eta^2\left(\eta^2 + \frac{t^2}{6} - k_A^2\right) d\eta$
B_2	cross section constant $\int_{\eta_{te}}^{\eta_{le}} t\eta\left(\eta^2 + \frac{t}{12} - k_A^2\right) d\eta$
C	$\frac{EB_2B'}{A}$
$\bar{C}$	$\frac{EB_2B'}{EI_1} \Big/ \frac{}{A}$
E	Young's Modulus
EI_1, EI_2	bending stiffness about major and minor principal axis of cross section respectively
G	Shear Modulus
GJ	St Venant's torsional stiffness
I_1, I_2	moments of inertia about major and minor neutral axes, respectively (both pass through centroid of cross sectional area effective in carrying tensions).
I_{2_e}	Moment of inertia of cross section about elastic axis
I_η, I_ξ	mass moment of inertia per unit length about η and ξ axes respectively
$\overline{I_\eta}$	$\frac{I_\eta}{\rho_o R^2}$
$\overline{I_\xi}$	$\frac{I_\xi}{\rho_o R^2}$
J	Torsional Stiffness constant $J = \frac{4I_1}{1 + \frac{16 I_1}{(\text{Area})(\text{Chord})^2}}$ (Ref 5 and 6)

M_1	Bending moment in flapwise direction
M_2	Bending moment in chordwise direction
Q	Torque about elastic axis at any cross section
R	Beam length
V_1, V_2	Shear load in flapwise and chordwise direction respectively
$\overline{X}$	$\frac{EB_1(\beta')^2}{EI_1}$
$\overline{Y}$	$\frac{E(B_2\beta')^2}{I_2 E I_1}$
a_n	mode constant for determination of frequency
e_A	distance between area centroid of tensile member and elastic axis, positive for centroid forward
$\overline{e}$	$\frac{e_A}{R}$
g	acceleration due to gravity
k_A	polar radius of gyration of cross-sectional area, effective in carrying out tensile stresses, about elastic axis
$\overline{k}_A$	$\frac{k_A}{R}$
l	length of blade segment
$\overline{l}$	$\frac{l}{R}$
m	mass of blade segment

p_x , p_η , p_ξ	total loadings per unit length in x , η, and ξ directions
q_x , q_η , q_ξ	total torque loadings per unit length in x , η, and ξ directions
t	thickness of cross section at any chordwise station
X	coordinate in direction of X axis measured from the root along the elastic axis
β	blade angle between major axis of cross-section and the "y" axis for $\phi = 0$, positive when leading edge is up.
β'	rate of twist of blade per unit length
$\Delta\beta$	increment in β between blade segments
γ	$\sqrt{\frac{EI_1}{EI_2}}$
δ_y , δ_z	displacement of elastic axis in "y" and " z " direction, respectively
δ_1 , δ_2	displacement of elastic axis in direction of minor and major principal axes of the cross-section, respectively
θ	total twist in blade between $x = 0$ and $x = R$
ξ , η	cross-sectional coordinate; η axis lies along major axis; ξ axis is perpendicular to major axis and passes through elastic axis.
λ^2	$\frac{\omega^2 \rho_0 R^4}{EI_1}$
ϕ	angle of twisting deformation, positive when leading edge is up
ρ	mass per unit length of blade
$\bar{\rho}$	$\frac{\rho}{\rho_0}$

Note: all zero subscripts refer to root section

Parameter Values for Beam Under Consideration

Values Independent of Twist

B_1	93.941	in^6
B_2	-11.50	in^5
E	10.5×10^6	lb/in^2
EI_1	$.7959 \times 10^6$	$lb\ in^2$
EI_2	32.81×10^6	$lb\ in^2$
G	4.0×10^6	lb/in^2
GJ	1.1864×10^6	$lb\ in^2$
I_1	.0758	in^4
I_2	3.125	in^4
I_{2e}	15.552	in^4
I_η	$.18723 \times 10^{-4}$	$lb\ sec^2/in^2$
I_ξ	38.4099×10^{-4}	$lb\ sec^2/in^2$
J	.2966	in^4
R	26.0	in
e_A	2.350	in
g	32.2	ft/sec^2
k_A	2.635	in
l	2.6	in
m	.00145	$lb\ sec^2/in$
ρ	.00055575	$lb\ sec^2/in^2$

Values which are dependent on twist

Total twist:	0^{o}	15^{o}	30^{o}
A (lb in^2)	1.1864×10^6	1.2699×10^6	1.5196×10^6
C (radians)	0	-.874780	-1.396937
θ (degrees)	0	15	30
θ (radians)	0	.2388	.4776
$\Delta\beta$ (radians)	0	.02388	.04776
β' (rad/in)	0	.00920	.01838

Non Dimensional Parameters

Values independent of twist

$\bar{I}_\eta$	.498356	$\times 10^{-4}$
$\bar{I}_\xi$	102.2392	$\times 10^{-4}$
$\bar{e}_A$	.09038	
$\bar{k}_A$	.1013	
$\bar{l}$	.1	
γ^2	.0243	
$\bar{\rho}$	1	

Values dependent on twist

For θ =	0°	15°	30°
$\bar{A}$	1.4906	1.59550	1.90440
$\bar{C}$	o	-.874780	-1.39694
$\bar{X}$	0	.12617	.50469
$\bar{Y}$	0	.0472554	.192792

EQUIPMENT AND PROCEDURE

The model used in the present investigation was made of 2024 T 4 Aluminum, machined from 6" x 1" stock. It was machined to within .015 inch of the given beam dimensions.

Four inches at the end of the model was left rectangular for mounting purposes (Fig. 1).

The bar was mounted with four bolts between two modified channel sections, which in turn were fastened to a double box section bolted to a structural member in the wall of the building. The double box section was made by welding 1/2" inch steel plates between the outer edges of the flanges of a 6 x 6, 5/8 inch steel I beam. (Figs. 3 and 4). The channel sections were later reinforced by welding a 0.5 inch steel gusset as shown in Fig. 3. This was done to observe the effect upon the natural frequencies of substantially stiffening the mounting. No measurable change in frequencies was noted. This provided some indication that the mounting was sufficiently rigid to give results that closely approached a true cantilever.

MB Vibration Test Equipment, Model T1 - 32034 was used to vibrate the beam. This machine has a frequency range of from two to 20,000 cycles per second. The vibrator itself was mounted to the floor and fastened to the beam with an aluminum tube. This tube was fastened to the vibrator with a flexure joint and to the beam with a universal joint (Figs. 3 and 4).

Two universal joints were used originally, one at each end of the aluminum tube, but this arrangement allowed too much slack in the connection. Two flexure joints were also tried in the same manner as the universals, but this arrangement

was too stiff to permit the beam sufficient freedom in torsion.

To obtain the desired twist, special fittings were made to fasten to each end of the bar so that it could be twisted about its elastic axis. A Riehle torsion testing machine of 120,000 in. lbs. capacity was used to twist the beam. The twisting rig as shown in Figs. 5 and 6 was used to transmit the torque.

The method of determining natural frequencies consisted of the following steps:

1) A frequency was approximately located by listening for and observing the amplitude maximum. In the case of the fundamental frequency this method provided an accurate answer by noting the frequency at which the measured maximum amplitude of the free end of the beam occurred.

2) The beam had been designed so that uncoupled natural frequencies of torsion and chordwise bending occurred in the vicinity of a natural uncoupled flapwise bending frequency. When the beam was being vibrated in the vicinity of a band of natural frequencies, fine sand of silicone flour was scattered over the surface of the beam. The frequency was then adjusted until sharp node lines appeared and concided with maximum amplitudes of vibration. The maximum amplitudes were recognized by first turning down the amplitude control of the vibrator until the sand or powder was barely agitated, then adjusting the frequency until the maximum agitation of the particles appeared. This method permitted the determination of amplitude maxima in a band of frequencies where sharp node lines did not disappear, but only shifted their positions. Where several maxima appeared in a band, the strongest was assumed to be the frequency of the flapwise bending mode. This assumption was made considering that a flapwise node was designed to occur in each band, and that due to the shape of the cross section, the flapwise vibration would be the dominant one.

It is the frequency change due to coupling effects as influenced by twist rather than the absolute value of the frequencies that is important in this report. Several factors occur in the experimental procedure which would tend to produce an experimental result different from one arrived at by calculations. Throughout the experimental runs, attention was directed toward keeping these factors constant.

The connecting rig between the beam and the shaker added end mass effect; this is discussed in the next section of this report. It was noted that varying the tightness of the bolts at the mounting even slightly could produce a slight variation in frequency. Of course, for all runs the beam was mounted as securely as possible so that the net effect of variations from one test to another was very small.

For the evaluation fo the analytic part of this report the Royal Precision Electronic Computer LGP-30, manufactured by the Royal McBee Corporation was to be used. A matrix program was set up as shown in the Appendix. The computer evidently could not handle the problem as it was programmed. A great deal of time had been spent on this part of the investigation and insufficient time remained to pursue it further.

RESULTS AND DISCUSSION

The effects of twist upon the natural frequencies of the beam are shown in Figs. 7 through 12. In Figs. 7 through 9, the absolute values of the natural frequencies are plotted versus the angle of twist. In Figs. 10 through 12, instead of absolute frequencies, the ratio of each frequency at any degree of twist to the corresponding value for the untwisted beam is plotted versus the angle of twist. The frequency ratios are grouped according to the assumed predominant motion, i.e. flapwise, chordwise or torsional.

Table I lists the uncoupled natural frequencies of the beam calculated on the basis of geometry and mass of the beam. These are compared with the corresponding natural frequencies observed when vibrating the untwisted beam. A coupled resonant frequency appears in the frequency spectrum corresponding to each calculated uncoupled natural frequency. It was assumed that the type of motion associated with each uncoupled natural frequency, remained as the predominant motion in the corresponding coupled natural frequency of the untwisted beam, and would continue to predominate as each frequency changed with twist.

The discussion of the effect of twist is based primarily on Figs. 10 through 12, the frequency ratio plots. In this discussion each frequency is identified by its predominant motion.

Twist has very little effect upon the fundamental frequency (first flapwise bending) of the beam. This frequency increases very slightly as the twist is increased through 30 degrees. The data point obtained at 40.4 degrees of twist indicates that there is a possibility of a more rapid rise in frequency as the twist is increased beyond this point.

The second flapwise frequency drops steadily as twist is increased to approximately 15 degrees; it remains constant as twist is increased further.

The third and fourth flapwise frequencies decrease as twist is increased to 10 degrees. For the next 10 degrees of twist, these frequencies rise slightly, then remain constant as twist is increased further.

The first torsional frequency, corresponding to the fourth natural coupled frequency of the beam, drops off rather rapidly as twist is increased to 15 degrees, it then decreases slowly as twist is further increased. The second torsional frequency decreases until about 15 degrees of twist is obtained, then tends to remain constant.

The third torsional frequency decreased to 15 degrees of twist then appeared to rise as twist was further increased. Data for the third torsional frequency was considered less reliable than the other data, because of the difficulty encountered in obtaining its resonance point and in obtaining sharp node lines.

Only the first chordwise frequency, corresponding to the third natural coupled frequency of the beam, was obtained. It dropped sharply until a twist of about 20 degrees was obtained; it then appeared to remain constant or rise slightly as further twist was introduced.

The shape and location of the node lines for the different frequencies are shown in Figs. 13 through 20. These were obtained when determining the natural frequencies. Although in some cases a band of frequencies occurred in which the node lines remained sharply defined and only changed their orientation and position with frequency, resonant peaks within the band were strong enough to permit determination of resonant frequencies. The occurence of frequency bands is

indicated in Figs. 13 through 20.

The shape and location of the node lines was significant in that they helped in the identification of the type of motion. It was noted that the node lines tend to move toward the free end of the beam as twist is increased to about 20 degrees. With further twist they remain relatively constant or even move slightly away from the free end. The position of the node lines in each group of frequencies reflects the flapwise bending mode occurring in that group.

The node line illustrations show the appearance of what was assumed to be resonant frequencies of plate bending. This assumption was made since no natural frequencies based on flapwise bending, chordwise bending, or torsion, were predicted to occur in this range. This plate bending first appeared near 300 cycles per second and became more pronounced as twist was increased. At high angles of twist, (20 to 30 degrees), it began at approximately 276 cycles and produced distinct node lines through a band of 400 cycles per second. Twist had little effect on the mean frequency of this mode as can be seen in Fig. 21.

This plate bending appeared again at about 680 cycles for a twist of 25.7 degrees, becoming evry distinct at a twist of 30.4 degrees. Another plate bending mode was seen to occur at 960 cycles and first appeared at a twist of 5.5 degrees.

Fortunately, the plate bending resonant frequencies appeared between the other bands of frequencies and though they undoubtedly influenced the shape of the node lines in the upper range of frequencies, it is felt that they did not greatly hinder the accurate determination of resonant frequencies in modes of vibration which are of interest in this paper.

In shaking the beam, certain frequencies above the fourth natural frequency

did not give distinct nodes. In these cases, the natural frequencies were plotted as a band rather than as a distintc point (Figs. 7 through 9). This difficulty was due not only to the proximity of the flapwise, chordwise, and torsional uncoupled frequencies, but also to the appearance of plate bending which was discussed above. Other inaccuracies were due to some unavoidable looseness in the vibrating mechanism, primarily the universal joint. This looseness also limited the frequency range obtainable, since the vibrating movement was lost in transmittal at high frequencies. The tube and fittings which connected the bean to the vibrator also added a slight end mass effect to the beam. By adding additional known mass weights to the end of the beam, it was determined that the effect of the vibrating rig reduced the fundamental frequency by 1.6 cycles per second. The data taken was not corrected for this effect, however, since the effect at higher frequencies was not known. The frequencies might also have been slightly low due to the impossibility of obtaining a perfectly rigid support at the root. The base of the beam however, was considered sufficiently rigid so that this effect was minor.

CONCLUSIONS

1. In all cases, the effect of bending-torsion coupling, independent of twist, appears to reduce the natural frequencies of the beam.

2. The fundamental frequency is relatively insensitive to twist, demonstrating only a slight rise as the angle of twist is increased.

3. All natural frequencies above the fundamental one are lowered as twist is increased to approximately 15 degrees.

4. Beyond 15 degrees of twist the natural frequencies are relatively independent of further twist.

REFERENCES

1. Houbolt, J.C., and Brooks, G.W., Differential Equations of Motion for Combined Flapwise Bending, Chordwise Bending, and Torsion of Twisted Nonuniform Rotor Blades, NACA TN 3905, 1957

2. Targoff, W.P., "The Associated Matrices of Bending and Coupled Bending-Torsion Vibrations." Journal of the Aeronautical Sciences, October, 1947

3. Targoff, W.P., "The Bending Vibrations of Twisted Rotating Beam." Proceeding of the Third Midwestern Conference on Solid Mechanics. University of Michigan Press, April 1957

4. Isakson, G., and Eisley, J.G., Natural Frequencies in Bending of Twisted Rotating Blades. University of Michigan Technical Report 2582-1-T April 1958

5. Roark, R.J., Formulas for Stress and Strain 1943 McGraw Hill Book Co. Inc. New York, London

6. Timoshenko, S., and Goodier, J.N., Theory of Elasticity. McGraw-Hill Book Company, Inc., 1951

7. Young, A.W., Elderton, E.M., and Pearson, K., "On the Torsion Resulting from Flexure in Prisms and Cross Sections of Uniaxial Symmetry", Drapers Co. Research Memoirs, Technical Series VII, 1918.

APPENDIX

METHOD OF ANALYSIS

The analysis is basically the one which is outlined in Ref. 3 and the Appendix of Ref. 4. It is extended to include torsional vibration and bending-torsion coupling and is applied to the non-rotating case.

The beam is divided spanwise into ten equal segments. The mass of each segment is assumed concentrated at its center, and the bending stiffnesses EI_1 and EI_2 and angle of incidence β are assumed constant between masses. The twist of the beam is accounted for by relative rotations of adjacent uniform bays (between masses) about a spanwise axis, the change in angle, $\Delta\beta$, being equal to the total twist in a segment and occuring just outboard of the mass.

With torsional motion included, the following quantities, at any point along the beam, may be expressed as a column matrix:

$$\{\Delta\} = \begin{Bmatrix} V_1 \\ M_1 \\ \delta_1' \\ \delta_1 \\ V_2 \\ M_2 \\ \delta_2' \\ \delta_2 \\ Q \\ \phi \end{Bmatrix}$$

The elements of this matrix vary from one station to the next along the beam in the following fashion: $\{\Delta\}_{n+1} = [R][E][F]\{\Delta\}_n$ where $[R][E][F]$ are 10 x 10 matrices representing linear relationships, described below, between the elements of $\{\Delta\}_n$ and corresponding elements in $\{\Delta\}_{n+1}$. Coupling effects are introduced into these relationships by consideration of the differential equations of coupled motion developed by Houbolt and Brooks in Ref. 1.

In the $[E]$ matrix which relates the $\{\Delta\}$ matrices across a weightless section, the elements are obtained as follows:

(a) $V_1^{(n+1)} = V_1^{(n)}$

(b) $M_1^{(n+1)} = M_1^{(n)} + V_1^{(n)}\ell$

From Ref. 1, at any station:

$$M_1 = EI_1(-v''\sin\beta + w''\cos\beta)$$
$$= EI_1(2\delta_2'\beta' + \delta_1'' + \delta_1\beta'^2 + \delta_2\beta'')$$
$$= EI_1\,\delta_1'' \quad (\beta = 0 \text{ for each station})$$
$$(EI_1\delta_1'')^{(n+1)} = M_1^{(n)} + V_1^{(n)}x$$

(c) $\delta_1'^{(n+1)} = \delta_1'^{(n)} - \frac{M_1^{(n)}\ell}{EI_1} - \frac{V_1^{(n)}\ell^2}{2EI_1}$

(d) $\delta_1^{(n+1)} = \delta_1^{(n)} - \delta_1'^{(n)}\ell + \frac{M_1^{(n)}\ell^2}{2EI_1} + \frac{V_1^{(n)}\ell^3}{6EI_1}$

(e) $V_2^{(n+1)} = V_2^{(n)}$

(f) $M_2^{(n+1)} = M_2^{(n)} + V_2^{(n)}\ell$

From Ref. 1, at any station:

$$M_2 = EI_2(v''\cos\beta + w''\sin\beta) - EB_2\beta'\phi'$$
$$= EI_2(\delta_2'' - 2\beta'\delta_1' - \beta''\delta_1 - \beta'^2\delta_2) - EB_2\beta'\phi'$$
$$= EI\,\delta_2'' - EB_2\beta'\phi'$$

For the untwisted section $\beta = 0$, but the second term in the above equation is not dropped since it represents the coupling between chordwise bending and twist which can only appear at this piont in the relationships. For this term, β must equal the amount of twist that actually exists in a segment having length x.

$$\left(EI_1\delta_2'' - EB_2\beta'\phi'\right)^{(n+1)} = M_2^{(n)} + V_2^{(n)}x \qquad (1)$$

(g) $$Q^{(n+1)} = Q^{(n)}$$

From Ref. 1, at any station:

$$Q = [GJ + EB_1(\beta')^2]\phi' - EB_2\beta'(v''\cos\beta + w''\sin\beta)$$

$$= [GJ + EB_1(\beta')^2]\phi' - EB_2\delta_2'' \quad (\beta = 0 \text{ for each station})$$

The β' appears in a coupling term and is retained as before.

$$[GJ + EB_1(\beta')^2]\phi' - EB_2\beta'\delta_2'' = Q^{(n)} \qquad (2)$$

Equations (1) and (2) are solved simultaneously for δ_2'' and ϕ; from δ_2'', δ_2' and δ_2 are obtained by integration.

(h)
$$\delta_2'^{(n+1)} = \frac{\left(AM^{(n)} + EB_2\beta'Q^{(n)}\right)\ell + \frac{AV_2^{(n)}\ell^2}{2}}{EI_2\left[A - \frac{(EB_2\beta')^2}{EI_2}\right]} + \delta_2'^{(n)}$$

(i)
$$\delta_2^{(n+1)} = \frac{\frac{\left(AM_2^{(n)} + EB_2\beta'Q^{(n)}\right)\ell^2}{2} + \frac{AV_2^{(n)}\ell^3}{6}}{EI_2\left[A - \frac{(EB_2\beta')^2}{EI_2}\right]} + \delta_2'^{(n)}\ell + \delta_2^{(n)}$$

(j)
$$\phi^{(n+1)} = \frac{Q^{(n)}\ell + \frac{EB_2\beta'}{EI_2}\left(M_2^{(n)}\ell + \frac{V_2^{(n)}\ell^2}{2}\right)}{A - \frac{(EB_2\beta')^2}{EI_2}} + \phi^{(n)}$$

where $A = GJ + EB_1(\beta')^2$

Equations (a) through (j) provide the elements of the $[E]$ matrix; these elements are put into non-dimensional form and the result is the 10x10 $[E]$ matrix whose terms are all zero except for the following:

$E_{11} = E_{22} = E_{33} = E_{44} = E_{55} = E_{66} = E_{77} = E_{88} = E_{99} = E_{1010} = 1$

$E_{21} = E_{65} = \bar{\ell}$

$E_{32} = E_{43} = E_{87} = -\bar{\ell}$

$E_{31} = -\frac{\bar{\ell}^2}{2}$

$E_{41} = \frac{\bar{\ell}^3}{6}$

$E_{42} = \frac{\bar{\ell}^2}{2}$

$E_{75} = -\frac{\gamma^2 \bar{\ell}^2}{2}\left(\frac{\bar{A}}{\bar{A}-\bar{Y}}\right)$

$E_{76} = -\gamma^2 \bar{\ell}\left(\frac{\bar{A}}{\bar{A}-\bar{Y}}\right)$

$E_{79} = -\bar{c}\gamma^2 \bar{\ell}\left(\frac{\bar{A}}{\bar{A}-\bar{Y}}\right)$

$E_{85} = \frac{\gamma^2 \bar{\ell}^3}{6}\left(\frac{\bar{A}}{\bar{A}-\bar{Y}}\right)$

$E_{86} = \frac{\gamma^2 \bar{\ell}^2}{2}\left(\frac{\bar{A}}{\bar{A}-\bar{Y}}\right)$

$E_{89} = E_{105} = \frac{\bar{c}\gamma^2 \bar{\ell}^2}{2}\left(\frac{\bar{A}}{\bar{A}-\bar{Y}}\right)$

$E_{106} = \bar{c}\gamma^2 \bar{\ell}\left(\frac{\bar{A}}{\bar{A}-\bar{Y}}\right)$

$E_{109} = \frac{\bar{\ell}}{\bar{A}-\bar{Y}}$

The quantities B_1 and B_2 are those defined by Houbolt and Brooks, Ref. 1, and were evaluated for the particular beam.

The elements of the $[F]$ matrix which relate the $\{\Delta\}$ matrices on either side of a concentrated mass are determined as follows:

$$V_i^{(n+1)} = V_i^{(n)} + m\ddot{\delta}_i + m e_A \ddot{\phi}$$

(a) $$= V_i^{(n)} + m\omega^2 \delta_i^{(n)} + m e_A \omega^2 \phi^{(n)}$$

(b) $$M^{(n+1)} = M_i^{(n)} + m k_i^2 \omega^2 \ell \delta_i'$$

The second term is one resulting from the entire segment's undergoing a change of slope when the beam bends.

k_1 = radius of gyration of a segment about a chordwise axis; m = mass of a segment.

(c) $$\delta_1'^{(n+1)} = \delta_1'^{(n)}$$

(d) $$\delta_1^{(n+1)} = \delta_1^{(n)}$$

$$V_2^{(n+1)} = V_2^{(n)} + m\ddot{\delta}_2^{(n)}$$

(e) $$= V_2^{(n)} + m\omega^2\delta_2^{(n)}$$

$$M_2^{(n+1)} = M_2^{(n)} + m k_2^2 \ddot{\delta}_2'$$

(f) $$= M_2^{(n)} + m k_2 \omega^2 \ell \delta_2'$$

The second term is a rotary inertia term as before;

k_2 = radius of gyration of a segment about a vertical axis; m = mass of a segment.

(g) $$\delta_2'^{(n+1)} = \delta_2'^{(n)}$$

(h) $$\delta_2^{(n+1)} = \delta_2^{(n)}$$

(i) $$Q^{(n+1)} = Q^{(n)} + m e_A \ddot{\delta}_1^{(n)} + m k_3^2 \ddot{\phi}^{(n)}$$

$$= Q^{(n)} + m e_A \omega^2 \delta_1^{(n)} + m k_3^2 \omega^2 \phi^{(n)}$$

where k_3 is the polar radius of gyration of the segment.

(j) $$\phi^{(n+1)} = \phi^{(n)}$$

Equations (a) through (j) are put into non-dimensional form and provide the elements of the $[F]$ matrix:

$$F_{11} = F_{22} = F_{33} = F_{44} = F_{55} = F_{66} = F_{77} = F_{88} = F_{99} = F_{1010} = 1$$

$$F_{14} = F_{58} = \bar{l}\,\bar{\rho}\,\lambda^2$$

$$F_{110} = F_{94} = \bar{\rho}\,\bar{l}\,\bar{e}_A\,\lambda^2$$

$$F_{23} = F_{67} = \frac{\bar{\rho}\,\bar{l}^3\lambda^2}{12}$$

$$F_{910} = (\bar{I}_\eta + \bar{I}_\zeta)\,\bar{l}\,\lambda^2$$

The $[R]$ matrix serves to rotate the coordinate axes through the angle $\Delta\beta$ and appears as follows:

$$R_{11} = R_{22} = R_{33} = R_{44} = R_{55} = R_{66} = R_{77} = R_{88} = \cos\Delta\beta$$

$$R_{15} = R_{26} = R_{37} = R_{48} = -\sin\Delta\beta$$

$$R_{51} = R_{62} = R_{73} = R_{84} = \sin\Delta\beta$$

$$R_{99} = R_{1010} = 1$$

The analysis then continues in the same manner as in Ref. 4, except that the matrices are now 10x10 and yield a 10x5 product when the boundary conditions at the tip are introduced.

The final results are obtained through evaluation of a 5x5 determinate. Introduction of trial values of λ, $[\lambda = f(\omega)]$, produce points which define the residual curve. Zero values of this curve define the natural frequencies.

TABLE I

COMPARISON OF COUPLED AND UNCOUPLED FREQUENCIES

Frequency (Cycles per second)		Type of Vibration
Uncoupled*	Coupled	
30.6	25.9	1st Flapwise
169	155	1st Torsion
195	163	2nd Flapwise
198	177	1st Chordwise
507	488	2nd Torsion
536	518	3rd Flapwise
844	---	3rd Torsion
1054	925	4th Flapwise

*Does not include the effect of end masses.

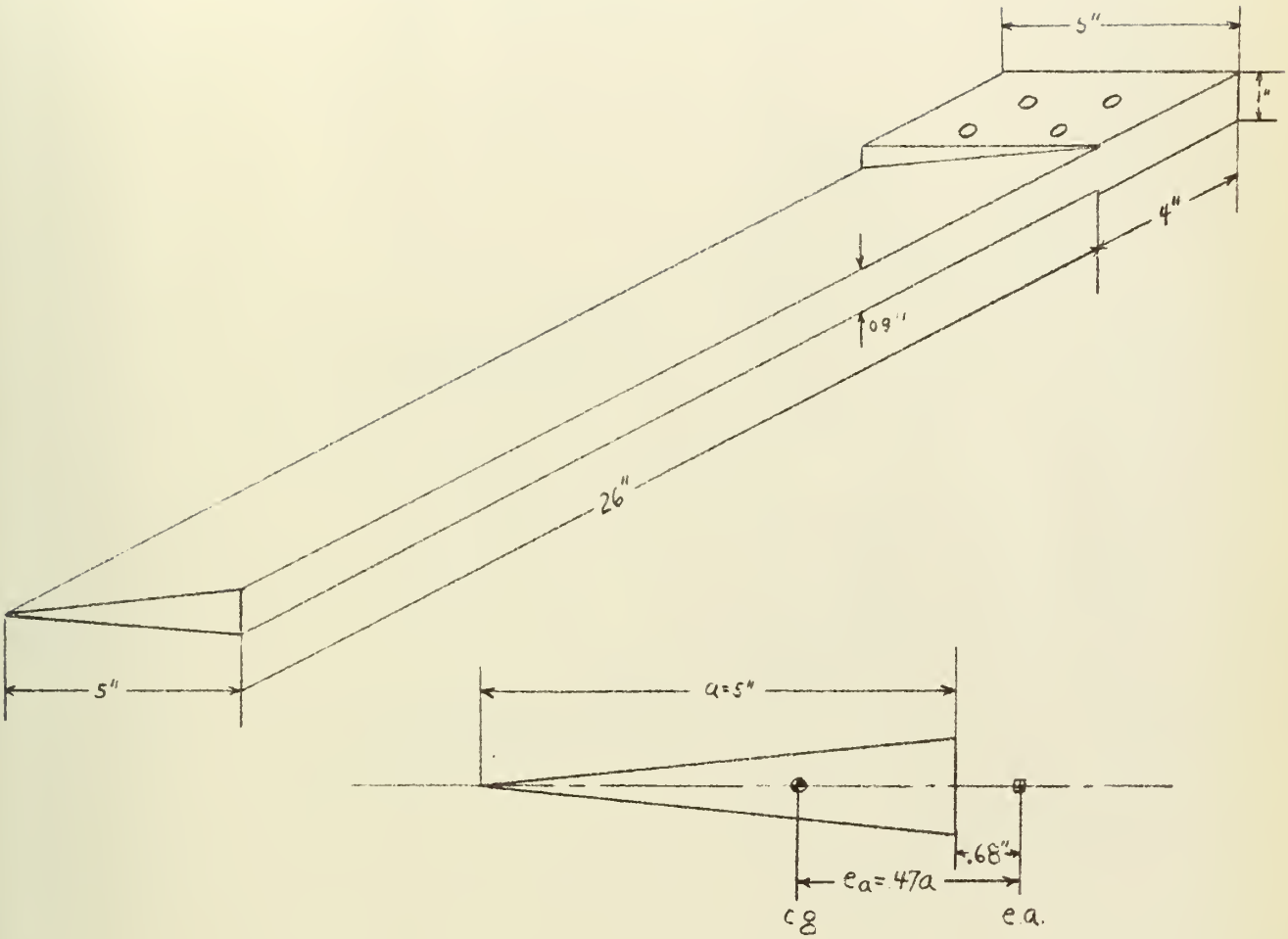

Fig 1

Sketch of Beam Showing Dimensions

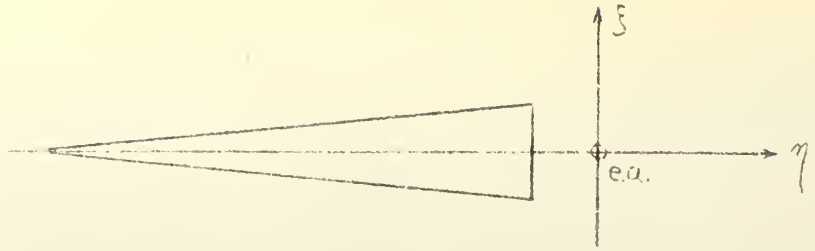

Local Cross Section Coordinates

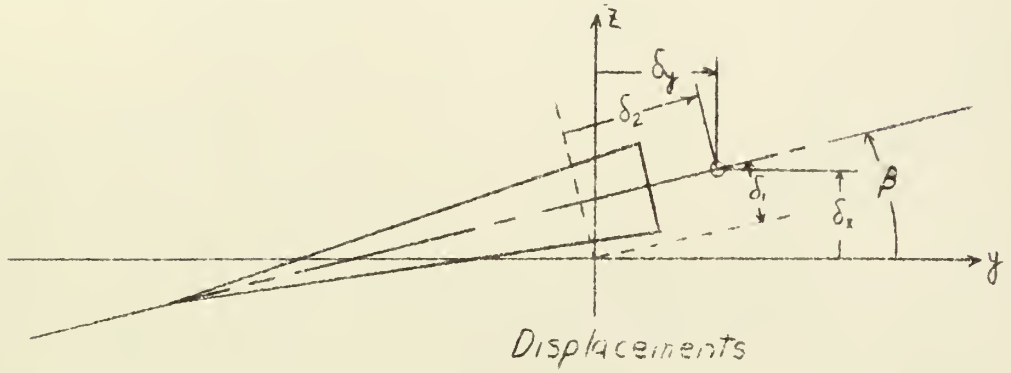

Displacements

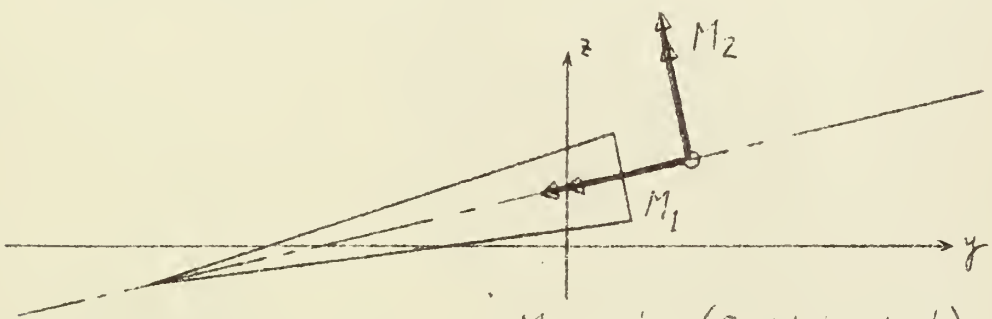

Moments (Right hand rule)

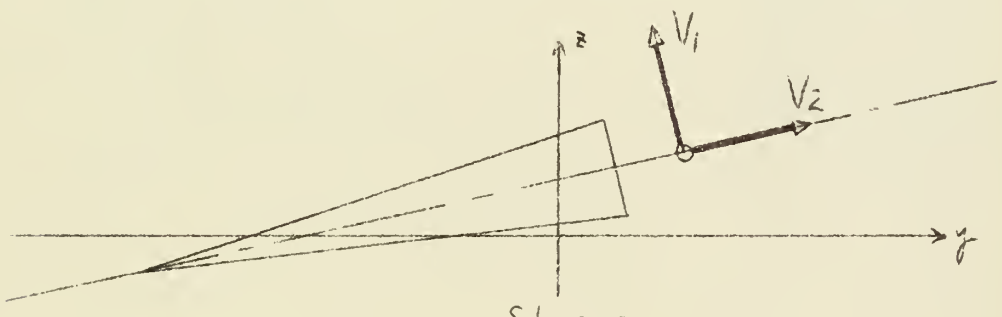

Shears

Fig 2
Coordinate System and Sign Convention
(Looking inward toward fixed end)

I Beam bolted to structural member in wall by 4 three-quarter inch bolts

I Beam: Flanges 5/16"
web 1/4"

Model Mounting:
Angle sections 1/2"
Outer gussets 1/4"
Inner gussets 1/2"

Note: Inner gussets were added to check rigidity

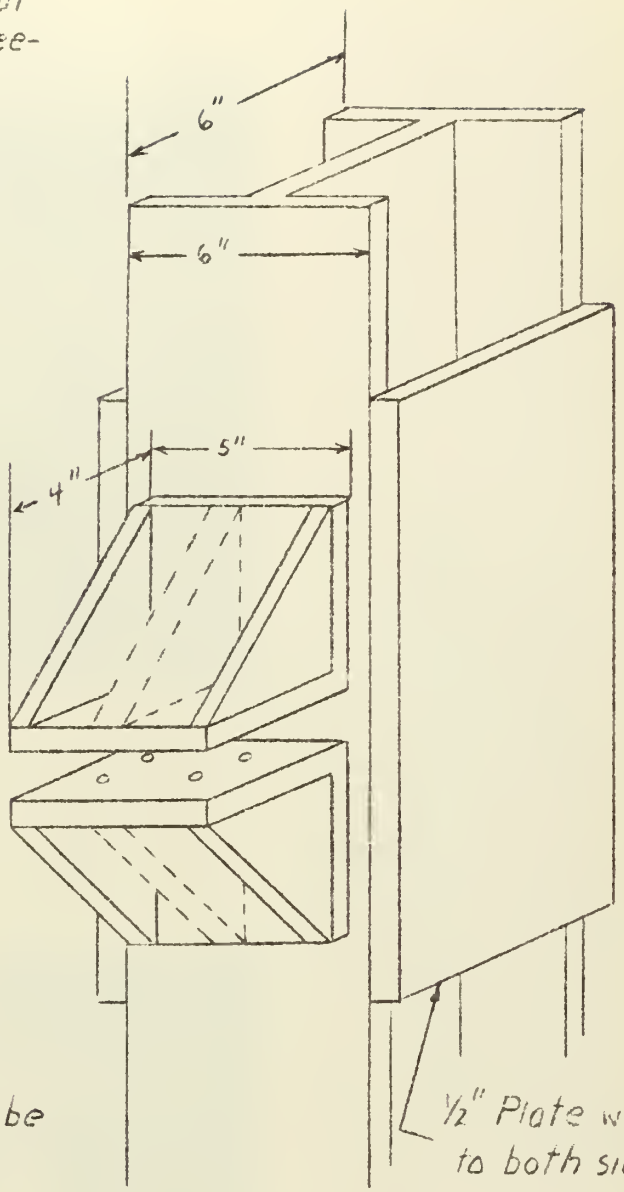

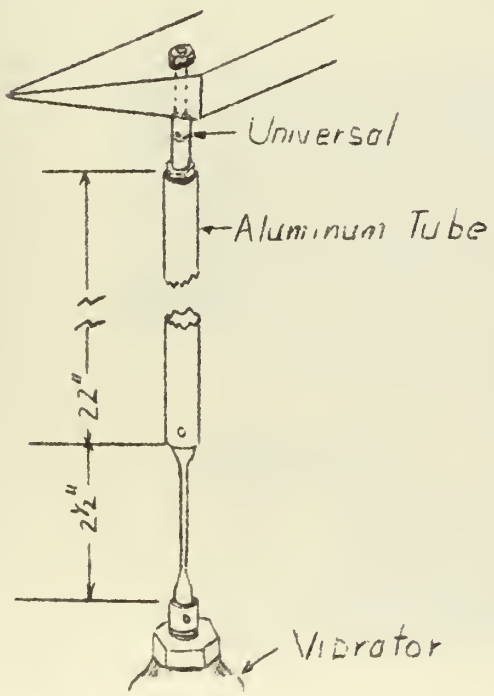

Fig. 3
Mounting Details

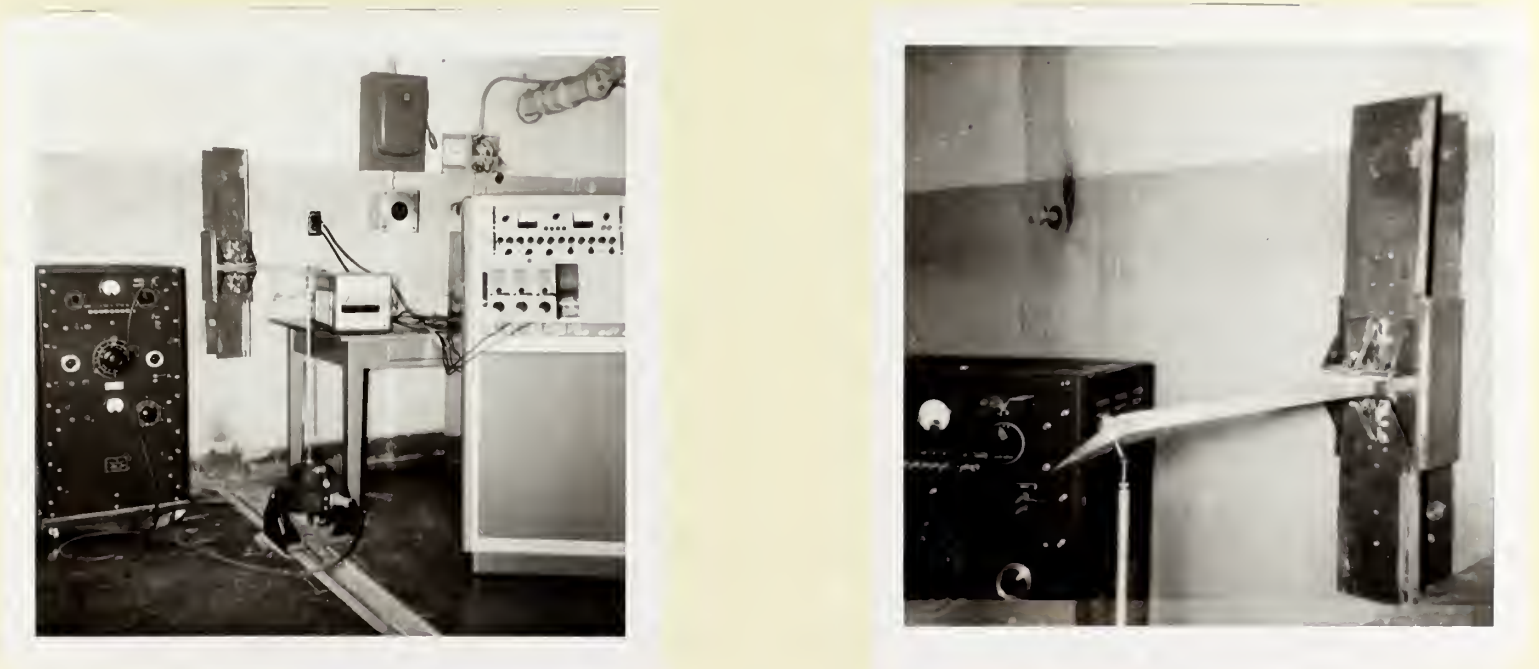

Fig. 4

Photographs of Vibrating Rig and Mounting

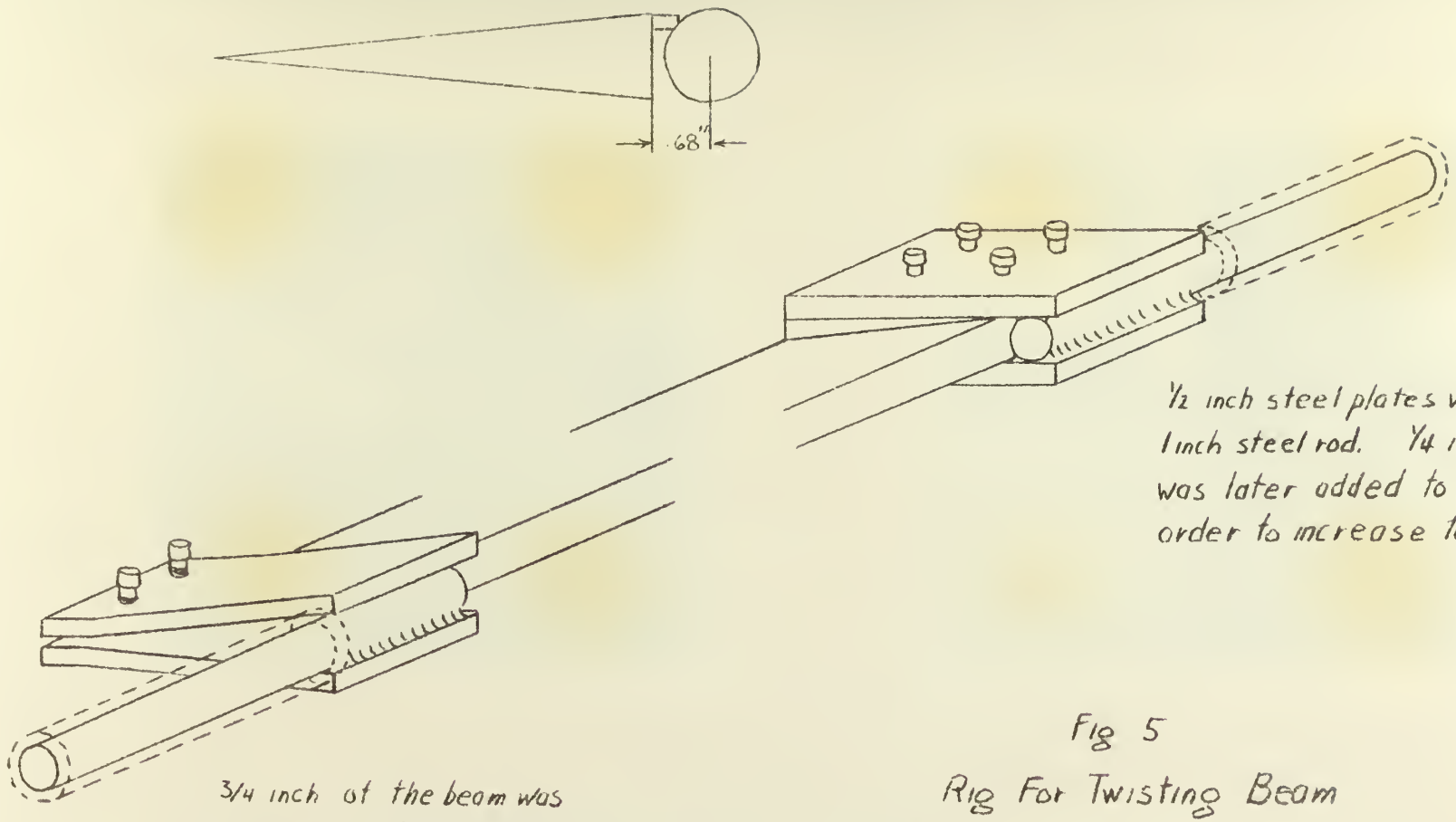

½ inch steel plates welded to 1 inch steel rod. ¼ inch sleeve was later added to the rod in order to increase torsional rigidity

3/4 inch of the beam was clamped in this attachment

Fig 5

Rig For Twisting Beam

Note: The center of the rod was located at the elastic axis of the beam. This permitted the beam to be twisted about its elastic axis.

Fig. 6

Photographs of Beam in Twisting Mechanism

Fig. 7

Effect of Twist on Natural Frequencies

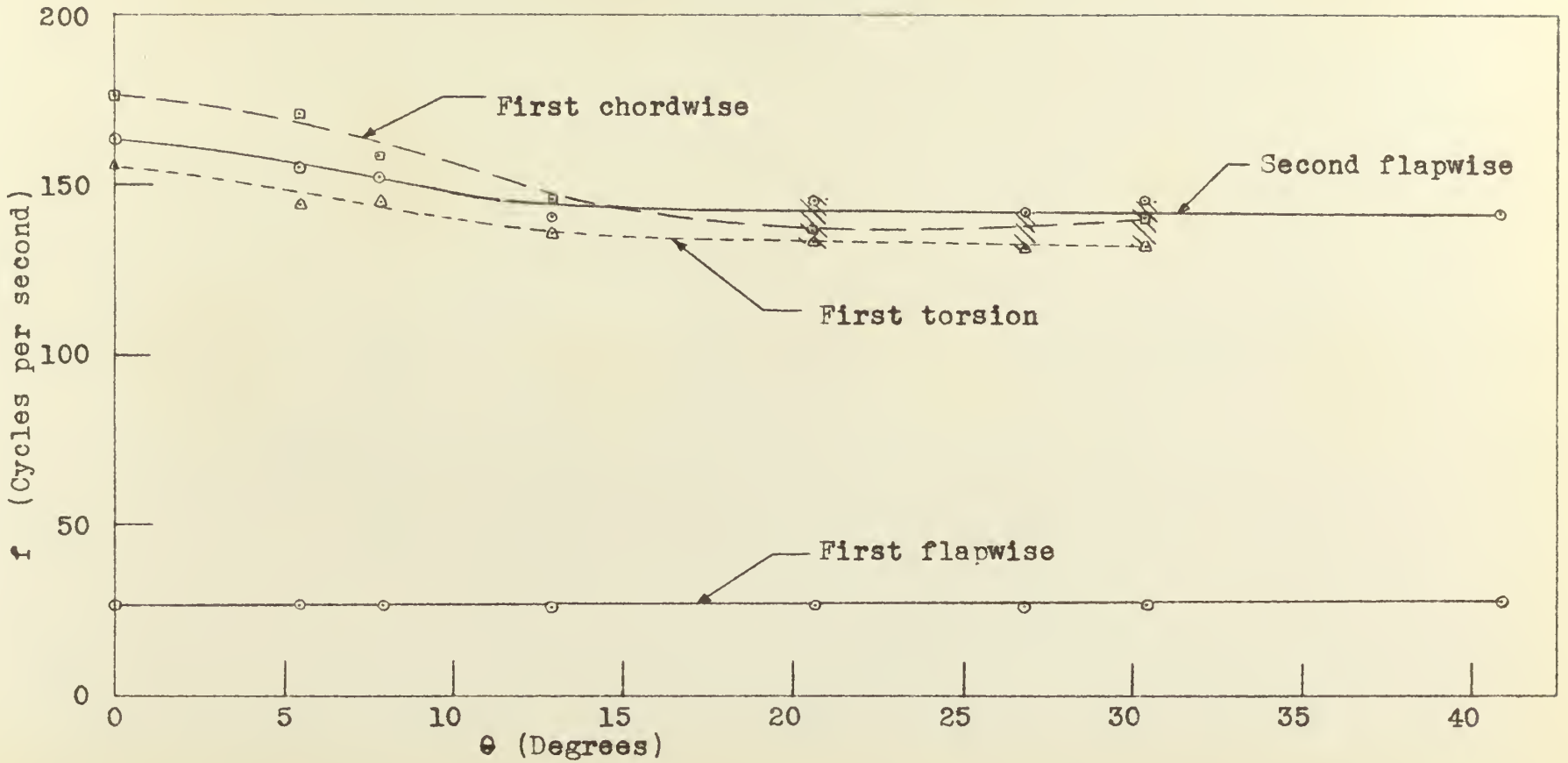

Fig. 8

Effect of Twist on Natural Frequencies

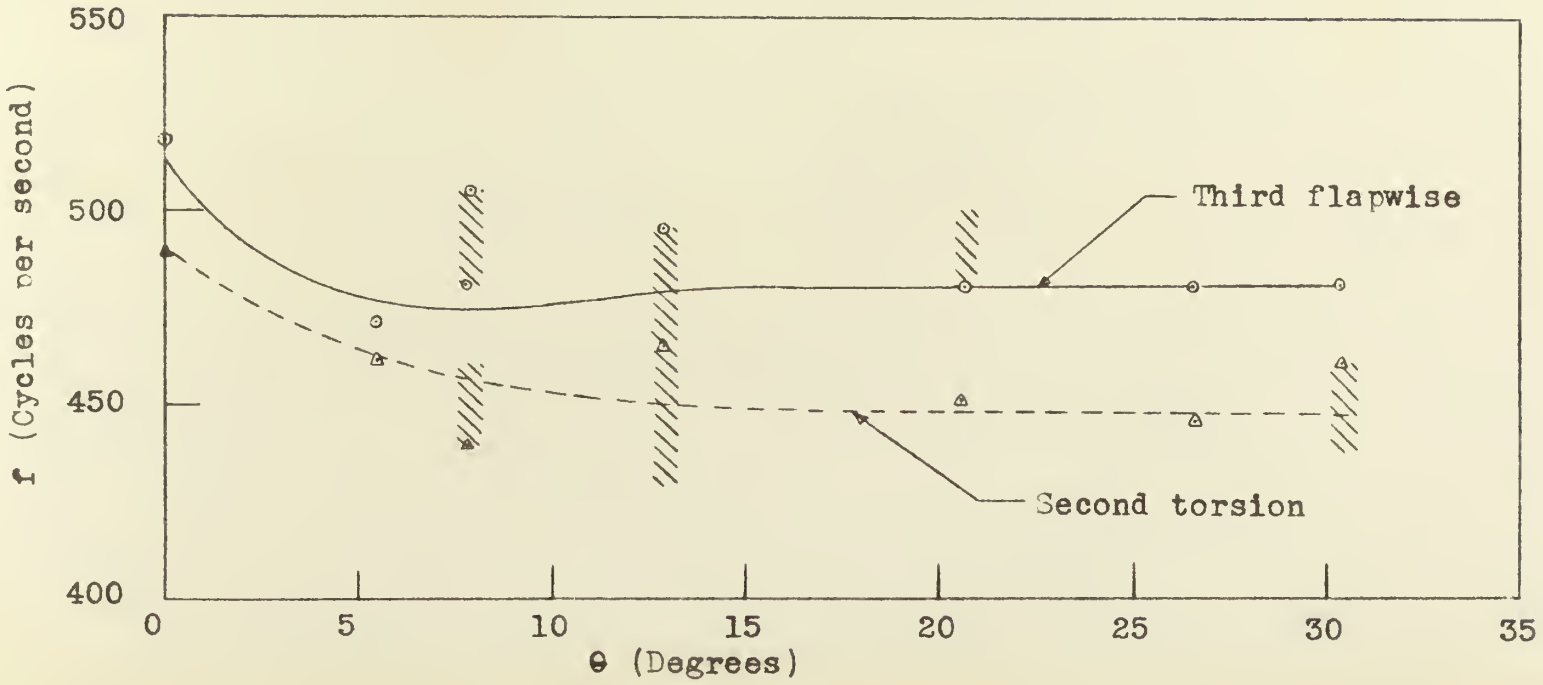

Fig. 9

Effect of Twist on Natural Frequencies

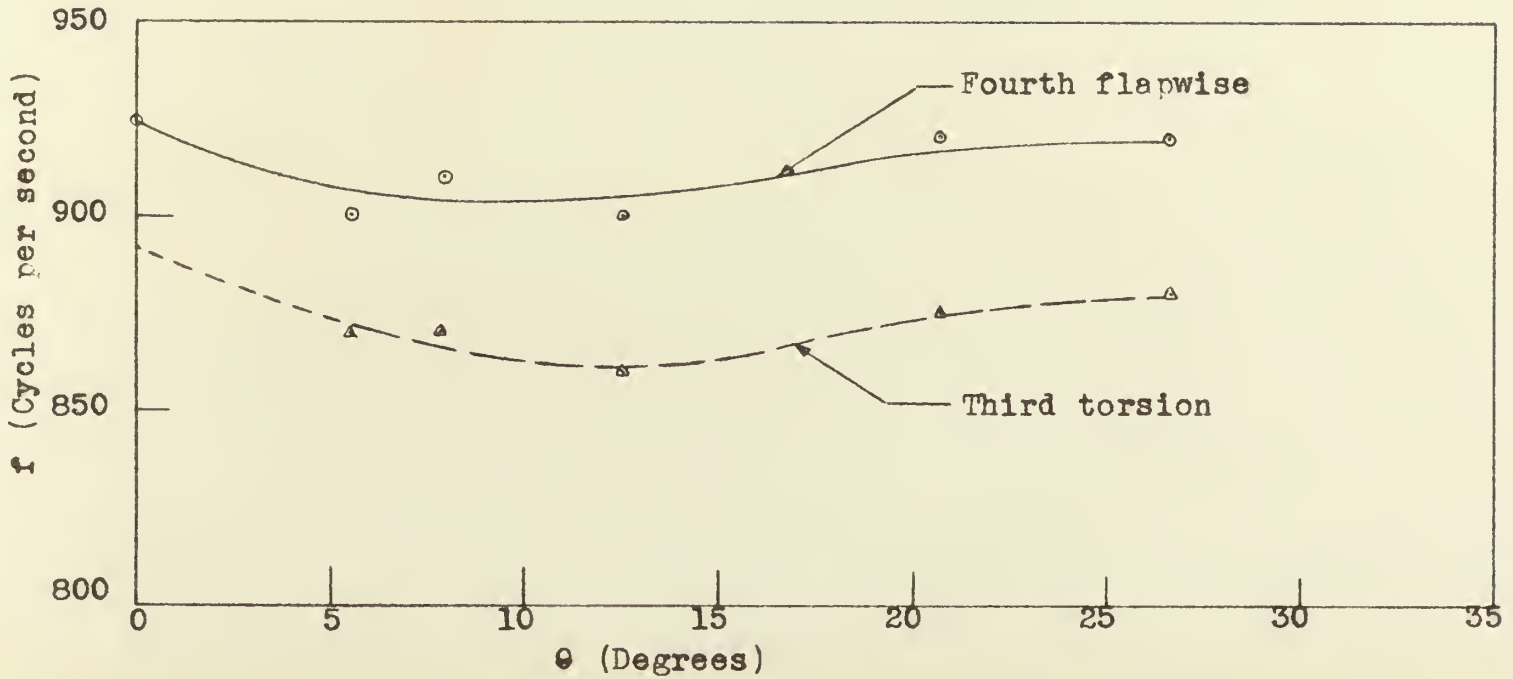

Fig. 10

Effect of Twist on Natural Frequencies

(Flapwise)

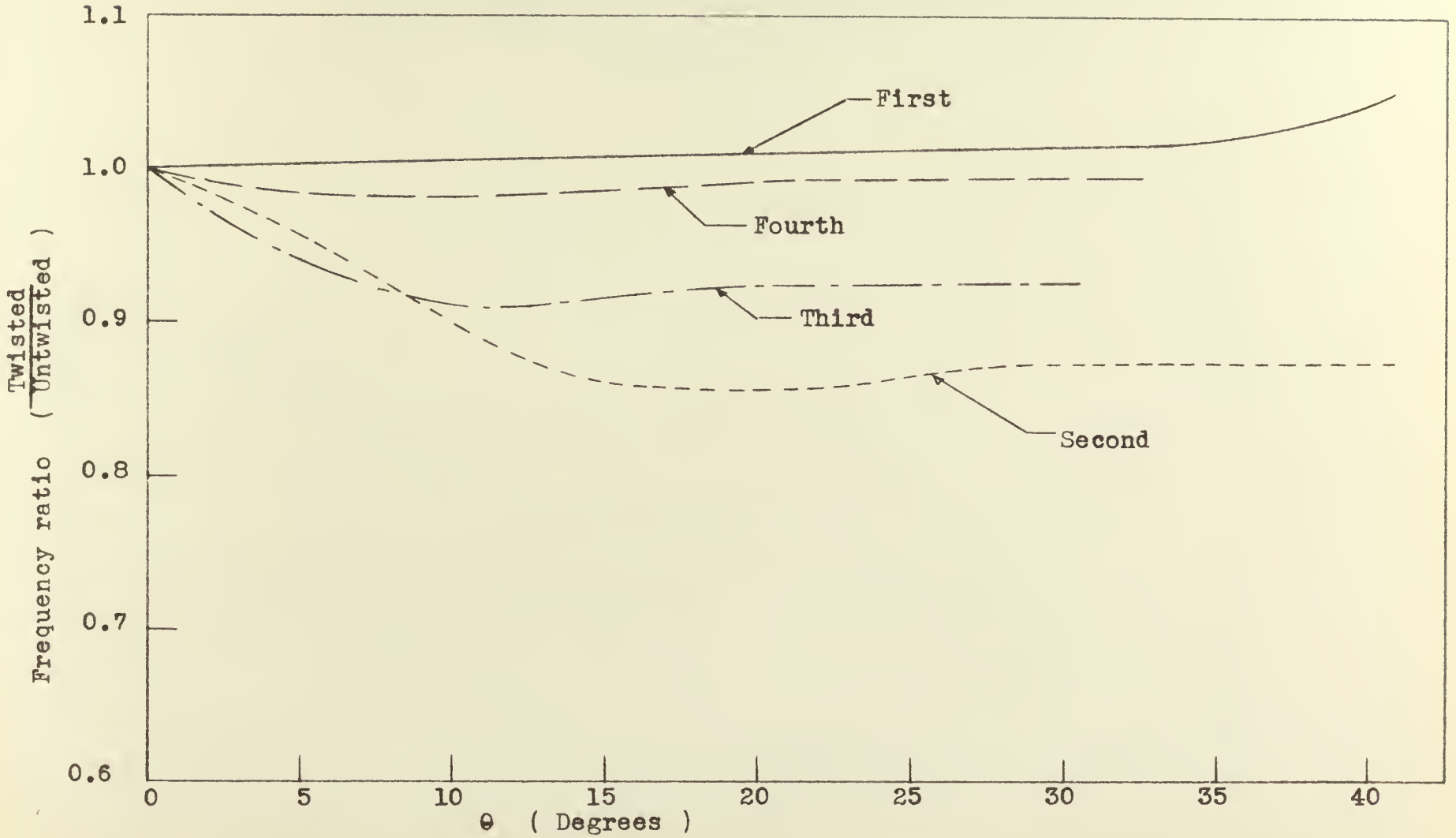

Fig. 11

Effect of Twist on Natural Frequencies

(Torsion)

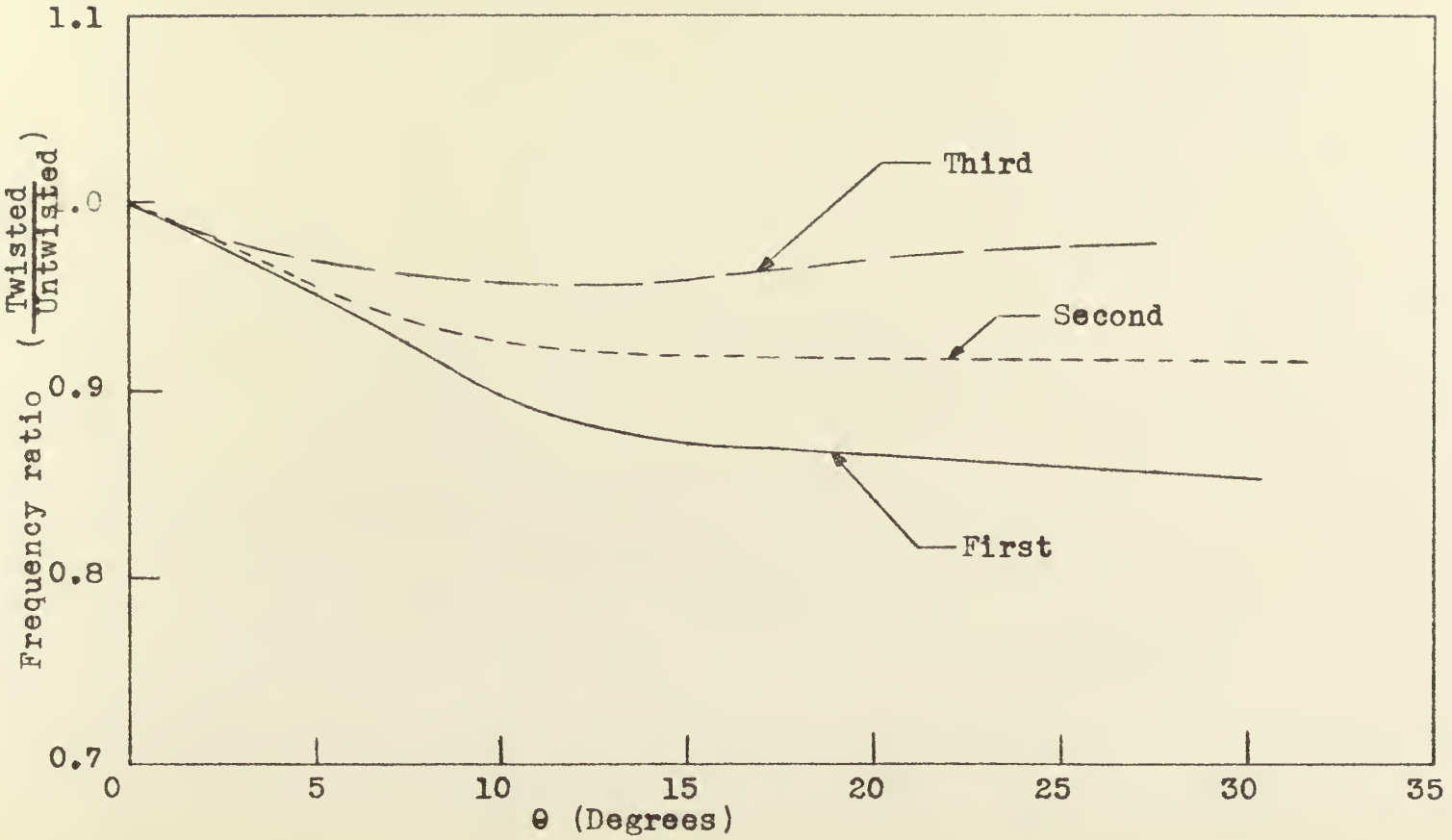

Fig. 12

Effect of Twist on Natural Frequencies

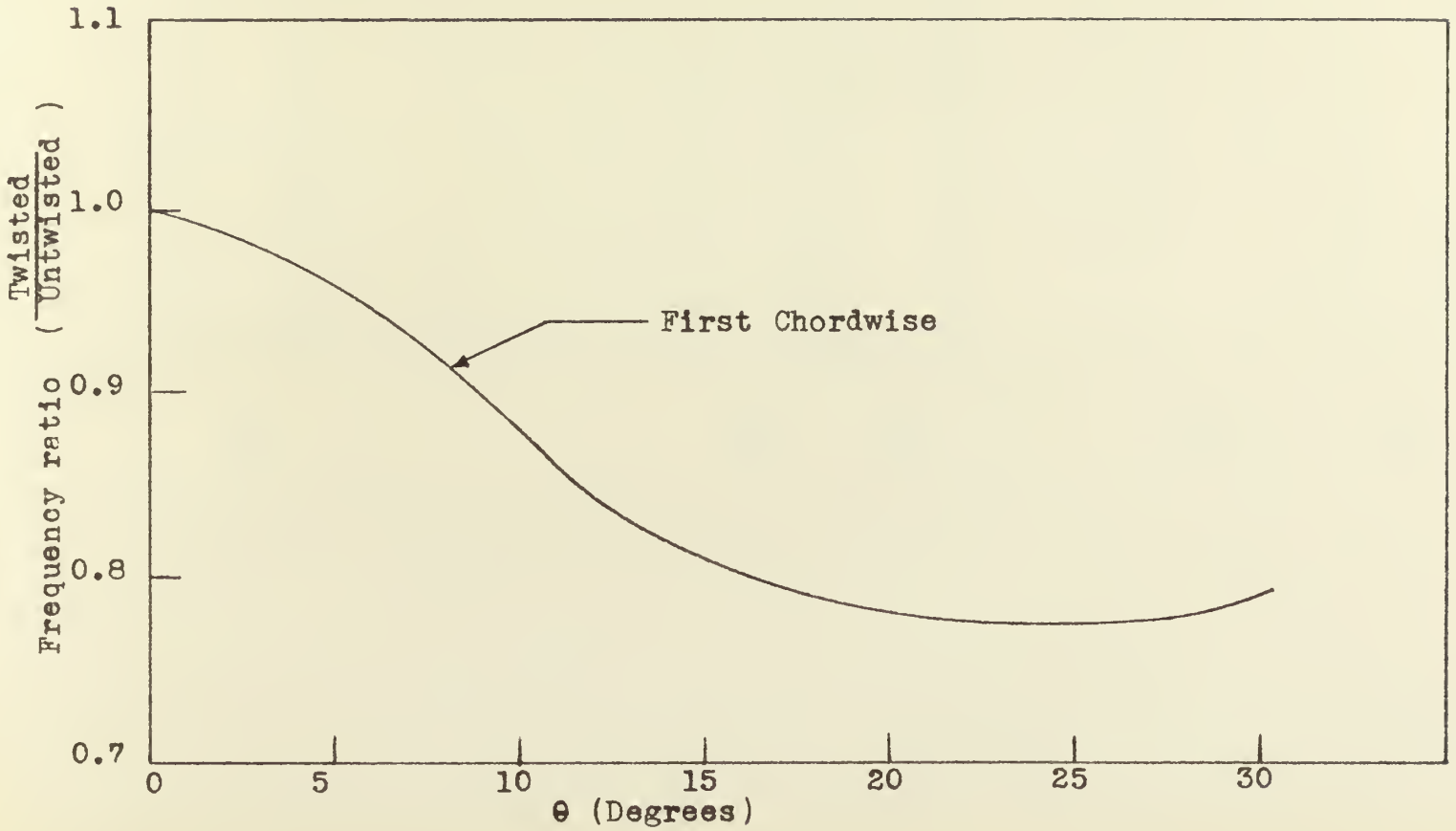

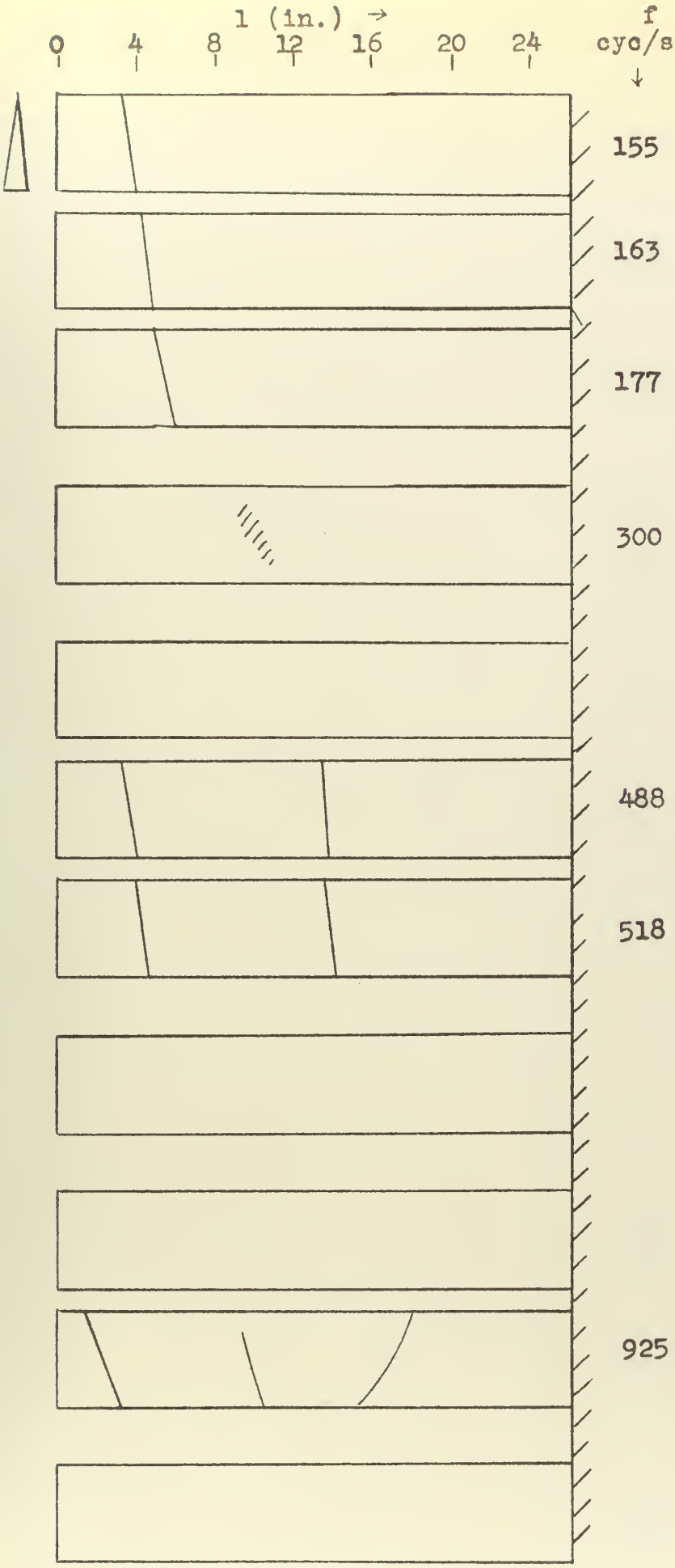

Fig. 13

Node Lines

$\theta = 0°$

Fund.Freq. = 25.9

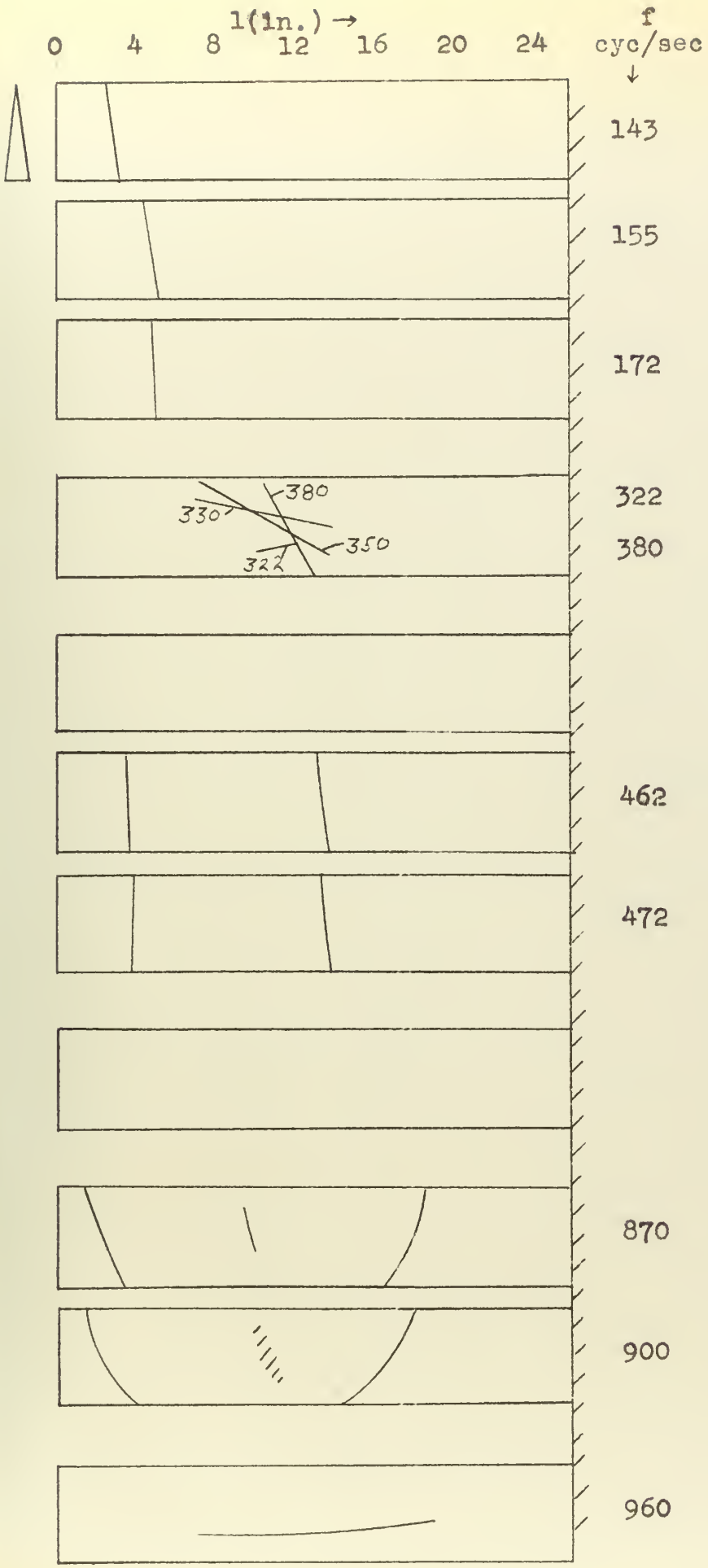

Fig. 14

Node Lines

$\theta = 5.5°$

Fund. Freq.=26.0

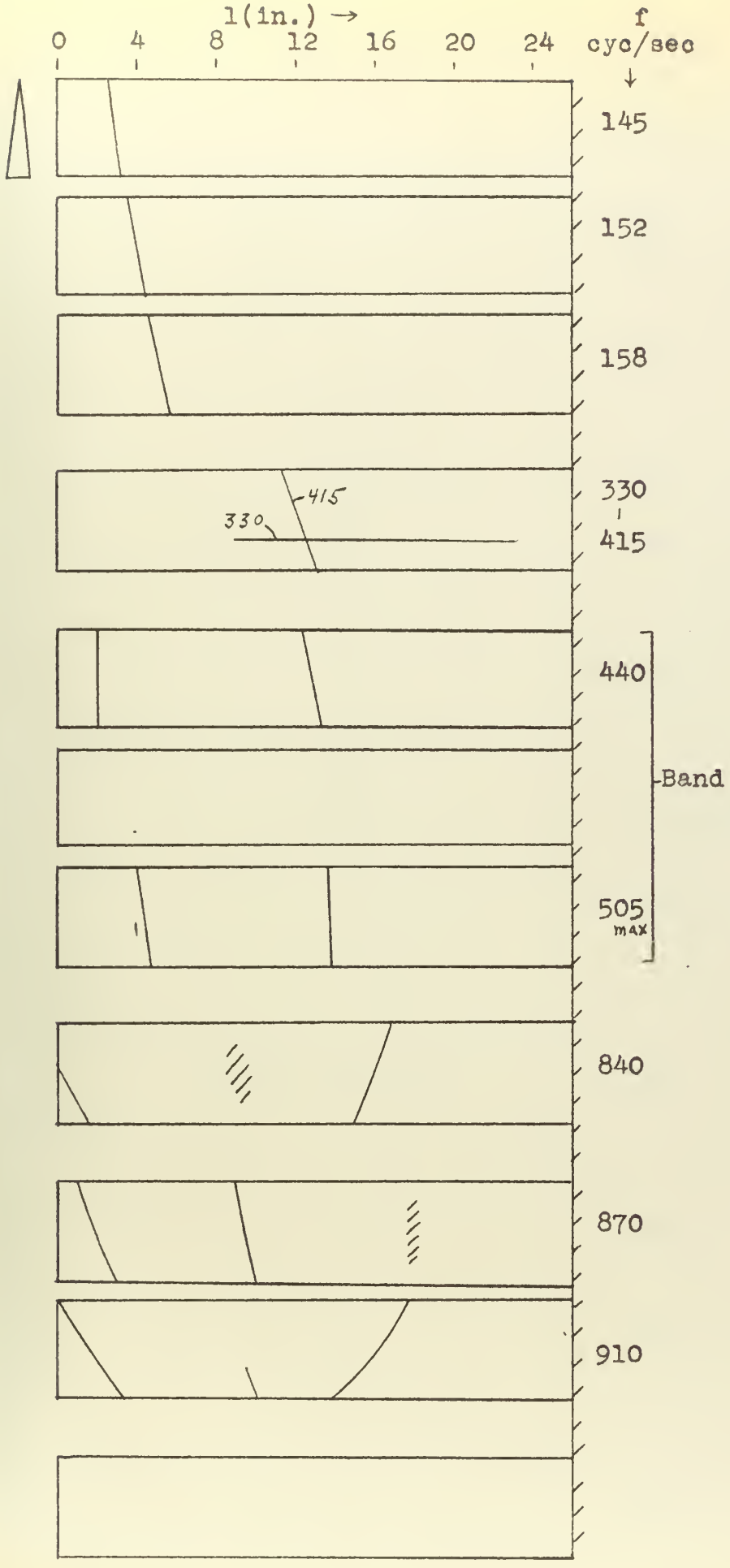

Fig. 15

Node Lines

$\theta = 7.9°$

Fund. Freq. = 26.1

Node at end of beam weakened at 460 cycles

Node at center of beam weakened at 480 cycles

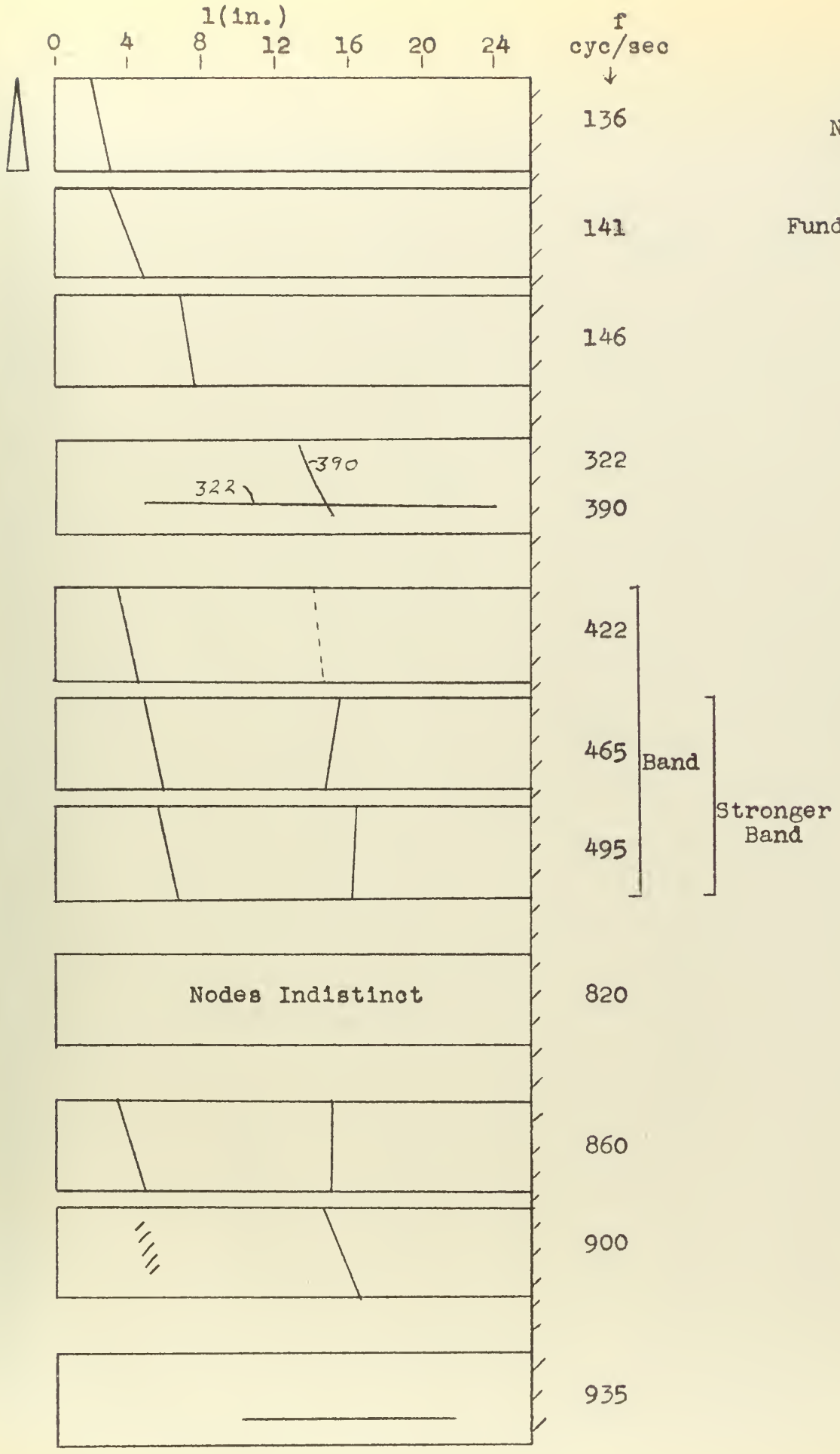

Fig. 16

Node Lines

$\theta = 12.9^{\circ}$

Fund. Freq. = 25.8

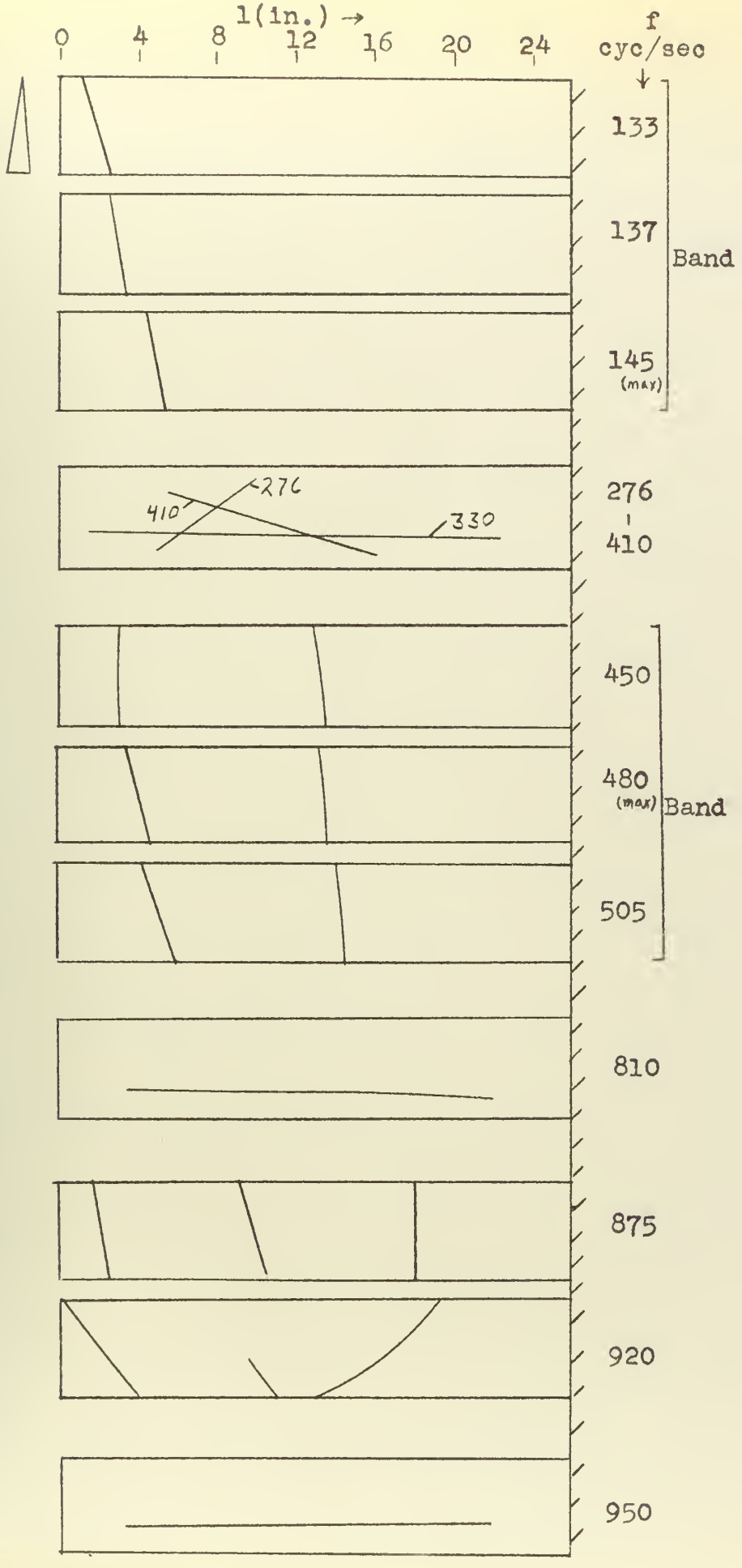

Fig. 17

Node Lines

$\theta = 20.7°$

Fund. Freq. = 26.0

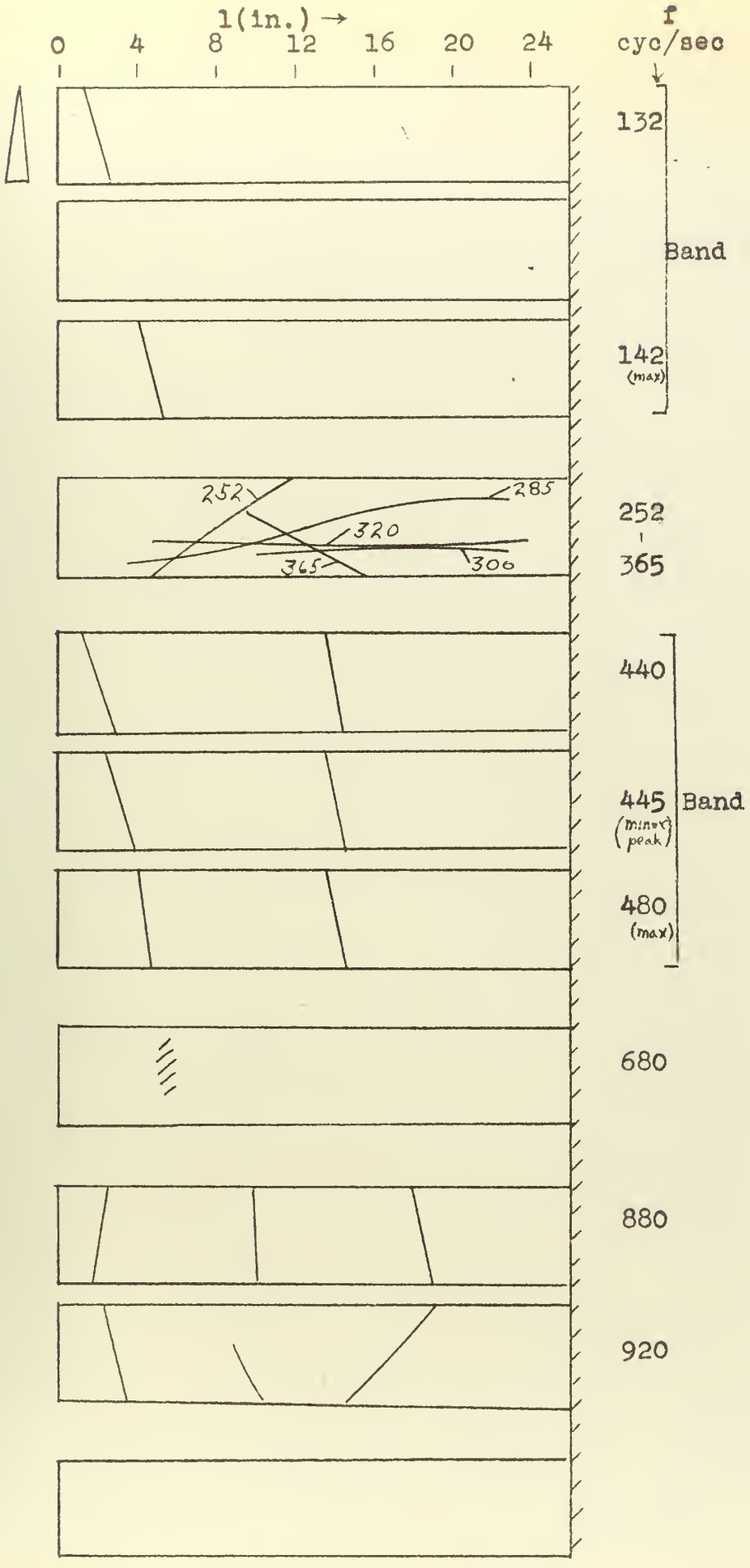

Fig. 18

Node Lines

$\theta = 26.7°$

Fund. Freq. = 25.7

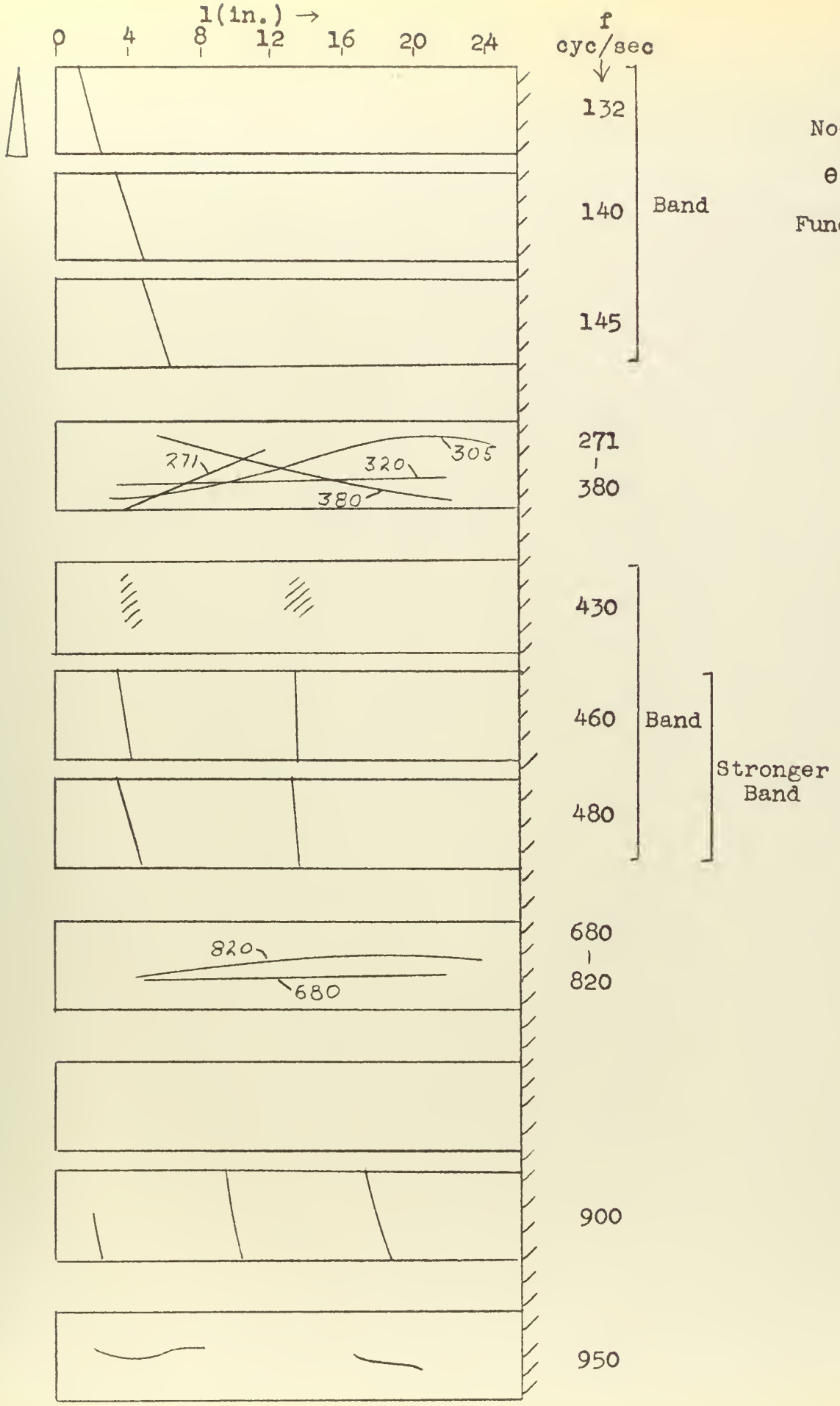

Fig.19

Node Lines

$\theta = 30.4°$

Fund. Freq.= 26.8

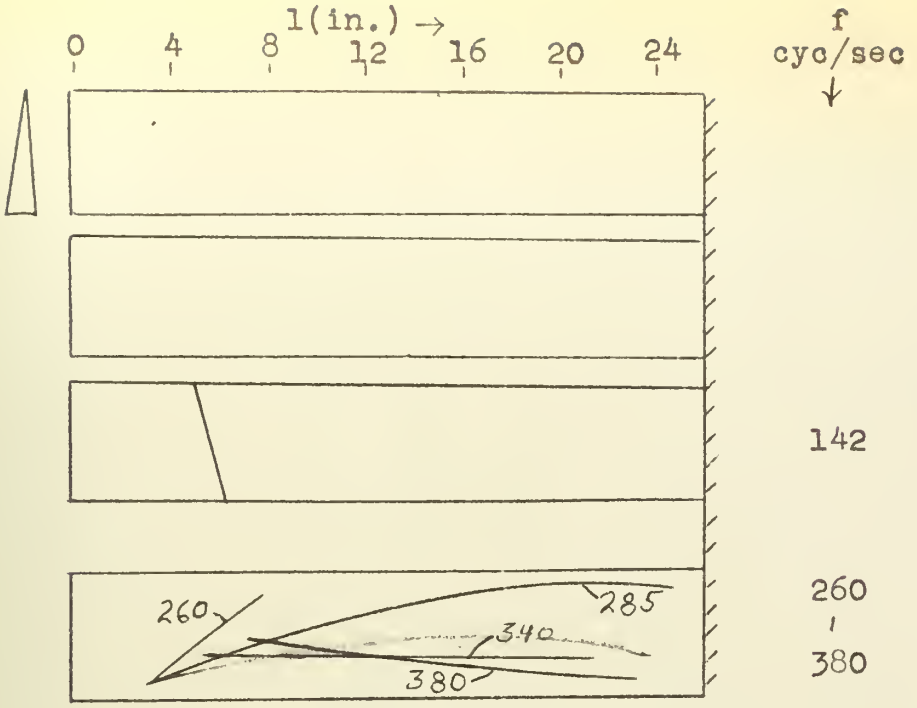

Fig.20

Node Lines

$\theta = 40.8°$

Fund. Freq. = 27.1

Fig. 21

Effect of Twist on Lowest Plate Bending Frequency

(Frequency plotted is that which produced a straight spanwise node line)